

Multi-Body Analysis of an Active Control for a Tiltrotor

G. L. Ghiringhelli P. Masarati¹ P. Mantegazza

*Politecnico di Milano
Dipartimento di Ingegneria Aerospaziale
Milano, 20158 Italy*

M. W. Nixon

*Army Research Laboratories
NASA Langley Research Center
Hampton, VA 23681*

Abstract

The design of advanced rotorcrafts requires the ability to analyse sophisticated, interdisciplinary systems to a degree of refinement that only recently has become achievable at a low price, thanks to the improvements in computer power. Multi-body analysis allows the detailed modeling of the kinematics as well as of the structural properties of rather sophisticated mechanical systems, such as helicopter rotors. When integrated with aeroservoelastic analysis, it represents a powerful tool for both the analysis and the design of aircrafts, with particular regard to rotorcrafts. An original multi-body formulation is presented, based on the direct writing of a system of differential-algebraic equations (DAE) that describe the equilibrium and the kinematic constraints of a structural system. The finite rotations, during the time-step integration of the initial value problem, are handled in an efficient manner by means of a technique called "Updated-Updated Rotations", an *Updated Lagrangian* approach that uses as reference the predicted configuration of the system. This allows to neglect the rotation perturbations in the computation of the Jacobian matrix, with considerable computational savings, while preserving the accuracy by consistently computing the residual. Control equations and the related unknowns are added, to model the control system to the desired level of refinement, from idealised control input/output signals, to each servosystem component. The numerical analysis of a tiltrotor configuration is proposed, based on an analytical model of the WRATS wind tunnel model. This is a 1/5 scale model of the V-22 tiltrotor

aircraft, currently tested in the Transonic Dynamic Tunnel (TDT) at NASA Langley. The control strategy is based on the Generalized Predictive Control (GPC) technique, with a Recursive Least Mean Squares (RLMS) on-line identification of an equivalent discrete linear system, that is used to design the adaptive controller. The rotor pitch controls are used as actuators. Different combinations of strain gages and accelerometers are used as sensor devices.

Keywords: MULTI-BODY ANALYSIS, PREDICTIVE CONTROL, TILTROTOR

Introduction

Aerospace vehicles must satisfy many requirements on performances, but also on handling qualities, comfort, environmental impact. Aircraft and rotorcraft designers are required a great effort to allow operations close to, or even inside, highly populated areas, and to provide the crew and the passengers a comfortable cockpit or seat, subject to as little vibrations and noise as possible. A viable answer to the latter requirements is represented by active control. The active control of rotorcraft has been investigated for a long time. Interest began early in the seventies, and grew continuously until today [16], [14]. Different techniques have been proposed to achieve the main goal of vibration and/or noise reduction. An exhaustive *resumé* of

¹Corresponding Author,
via La Masa 34, 20158, Milano
Tel.: ++39(02)3933-2393
Fax: ++39(02)3933-2334
E-mail: masarati@aero.polimi.it

the state of the art and of the most promising developments can be found in Ref. [5]. Vibrations in the airframe can be reduced both by cancelling their effects or by eliminating their source, namely periodical blade airloads. In this paper the second approach is investigated. Basically, rotorcraft vibrations originate from the discrete nature of the rotor, that is made of a finite number of blades. This results in time-dependent aerodynamic loads in forward flight, related to the different airstream speed experienced by the blade when it is advancing and retreating, that results in dynamic stall and in reverse flow at the inner part, even for comparatively low advancing ratios. Noise and vibrations are also originated by the vortex sheet shed by a blade, when impacting on the following one (Blade-Vortex Interaction, or BVI). The loads generated by a rotor blade can be modified by acting on the blade pitch, both directly (i.e. by changing the pitch of the whole blade by means of the swashplate or other pitch control device) or indirectly (i.e. by actuating a trailing edge flap, that induces a blade twisting moment). Rotorcraft active control has been traditionally and naturally oriented towards Higher Harmonic Control-like (HHC) approaches ([10], [3], [13] among the others) because the blade pitch actuation mechanism represents an easy and cheap way to apply the required control power directly to the blade and requires limited additional power. Moreover, the periodic nature of the blade vibratory loads allow an easy design of harmonic control laws. Both open- and close-loop control have been investigated, the latter often being used in conjunction with the adaptive, in-line identification of a linearised, frequency domain transfer function of the rotorcraft. It suffers from some disadvantages, mainly related to the periodic nature of the control input and to the comparatively low maximum actuation frequency, resulting in limited flexibility. The Independent Blade Control (IBC) is complementary to the HHC. Each blade is considered as an independent system, and is controlled by an independent controller [9]. This technology is not as mature as HHC; the main problem that has to be faced is a viable and efficient means to deliver the control power into the rotating system [5], [8]. A different approach is used in the present work, based on the Generalised Predictive Control technique [2], [4], [11]. There is no exploitation of the periodic nature of the rotor dynamics as a means to generate

periodic control forces. On the contrary, the rotor, and the whole rotorcraft, are considered as a black-box that is identified on-line as a discrete-time, locally constant-coefficient linear system. The slow, long term variation of the system coefficients is accounted for by the recursive implementation of the identification. Based on the identified system, the response is predicted, and the control signal is designed by enforcing the desired behaviour of the controlled system. The paper first presents the predictive control theory that is used in the design of the control. A brief description of the multi-body formulation that is used for the analytical model of the tiltrotor is given, followed by a comparison with numerical and experimental results of the WRATS tiltrotor wind tunnel model [7]. This model, controlled by a proprietary implementation of the HHC called MAVVS, has been tested by Bell Helicopter at NASA Langley Research Center (LaRC) [15]. Finally the numerical results of the proposed control technique are illustrated and discussed.

Discrete Control

Discrete Time Equation. A discrete time, Auto-Regressive, Moving Average, with eXogenous input (ARMAX) equation has the form:

$$y(k) = a_1 y(k-1) + \dots + a_p y(k-p) + b_0 u(k) + \dots + b_p u(k-p) + e(k) + c_1 e(k-1) + \dots + c_p e(k-p)$$

where $y(t)$, $u(t)$ are the output and input arrays at time t , $e(t)$ is the error array at time t , a_j , $j = 1, p$, b_j , $j = 0, p$ and c_j , $j = 1, p$ are the matrices of a p -order, time-independent, linear discrete system. The number of equations is represented by the number of outputs m ; matrices a_i are $m \times m$, as matrices c_i are. Matrices b_i are $m \times n$, being n the number of inputs. Usually the matrices of the system are unknown, only measures of inputs and outputs being available; the error can be measurable or not, depending on its nature. An unmeasurable, biased error is assumed unless otherwise stated.

System Identification. The yet unknown system matrices can be stacked in a matrix Θ , while the observations can be stacked in an array $\varphi(k)$, as follows:

$$\Theta = [a_1, \dots, a_p, b_0, \dots, b_p, c_1, \dots, c_p]$$

$$\varphi = \begin{bmatrix} y(k-1)^T, \dots, y(k-p)^T, \\ u(k)^T, \dots, u(k-p)^T, \\ e(k-1)^T, \dots, e(k-p)^T \end{bmatrix}^T$$

The predicted output is:

$$\hat{y}(k) = \Theta \varphi(k) \quad (1)$$

and the difference between the current and the predicted output represents the error at the current time step, which is unknown by definition. Matrix Θ depends on k as far as it is estimated from a finite set of measures; it approaches the exact value provided the true system has the form of the assumed model. Equation 1 gives a means to estimate the error at every time step in a recursive manner. The error may be due to unmeasured disturbances, errors in measures, and errors in the parameters of the model (type, order, and so on):

$$e(k) = y(k) - \hat{y}(k)$$

The observations at time steps ranging from i to j can be stacked by columns: $y = y(i:j)$, $\varphi = \varphi(i:j)$, $e = e(i:j)$, giving:

$$e = y - \Theta \varphi \quad (2)$$

where the expected output that results from the yet to be identified system, $y_e = \Theta \varphi$, is used. If the error is unbiased, Equation 2 does not depend on the error itself (the error does not participate in array φ) and thus Θ can be solved for a finite set of measures to determine the optimal value of the unknown parameters. In case of biased error, instead, it can be determined by recursively adding columns to Equation 2, and using each parameter estimate to compute the current estimate of the error. A global measure of the error is:

$$J = ee^T$$

The minimisation of J with respect to Θ gives a least squares fit of the system:

$$\Theta = y\varphi^T (\varphi\varphi^T)^\dagger$$

where the \dagger denotes the pseudo-inversion, that is required in case the system is only semi-definite. In this case, the excitation is not persistent, or the system is not completely controllable.

Recursive Implementation. The recursive expressions of matrices $\varphi\varphi^T$ and $y\varphi^T$ are:

$$(\varphi\varphi^T)_{j+1} = (\varphi\varphi^T)_j + \varphi(k+j)\varphi(k+j)^T$$

and:

$$(y\varphi^T)_{j+1} = (y\varphi^T)_j + y(k+j)\varphi(k+j)^T$$

The inverse of matrix $\varphi\varphi^T$ can be directly updated instead of factorising the updated matrix, by using the LDL^T factorisation, since the matrix is symmetric and positive definite or semidefinite in the worst case; the positive definiteness can be artificially enforced. In this way, the numerical loss of accuracy can be reduced while improving the efficiency of the computation. The recursive algorithm is:

$$\begin{aligned} \Phi(k)^\dagger &= \mu\Phi(k-1)^\dagger + \varphi(k)\varphi(k)^T \\ \psi(k) &= \mu\psi(k-1) + y(k)\varphi(k)^T \\ \Theta(k) &= \psi(k)\Phi(k) \\ e(k) &= y(k) - \Theta(k)\varphi(k) \end{aligned}$$

The first two above equations update the matrices $\Phi(k) = \left(\sum_{j=1,k} \varphi(j)\varphi(j)^T\right)^\dagger$ and $\psi(k) = \sum_{j=1,k} y(j)\varphi(j)^T$, where a forgetting factor μ has been used to identify a comparatively slowly time-varying system. The third equation updates the estimate of the system parameters; the last equation estimates the error at the current step. Artificial stabilisation of the moving average part of the system is required, since unstable error dynamics, that can occur during the identification especially in the initial phase, have no physical meaning [1].

Output Prediction. As soon as an estimate of the system to be controlled is available, either by parametric modelling or by black box identification, the horizon of the prediction can be easily extended. The predicted value at time $t = k + 1$ is:

$$\begin{aligned} y(k+1) &= a_1y(k) + \dots + a_p y(k-p) \\ &+ b_0u(k+1) + \dots + b_p u(k-p+1) \\ &+ c_1e(k) + \dots + c_p e(k-p+1) \end{aligned}$$

the difference between the predicted and the actual values being the error. By substituting the predicted value of the output at time $t = k$, it becomes:

$$\begin{aligned} y(k+1) &= a_1^1y(k-1) + \dots + a_p^1y(k-p) \\ &+ b_0^1u(k+1) + b_0^1u(k) + \dots + b_p^1u(k-p) \\ &+ c_1^1e(k-1) + \dots + c_p^1e(k-p) \end{aligned}$$

where the new system matrices are recursively defined as:

$$x_i^0 = x_i, \quad x_i^j = a_1^{j-1}x_i^0 + x_{i+1}^{j-1}, \quad x_{p+1} = 0$$

where x stands for a , b , and c , respectively. The predicted error at step k and beyond is assumed to be null since the error is assumed to be uncorrelated with the outputs, the inputs and the

past errors, while the estimates of the output are supposed to be exact. The predicted value at time $t = k + j$ becomes:

$$\begin{aligned} y(k+j) &= a_1^j y(k-1) + \dots + a_p^j y(k-p) \\ &\quad + b_1^j u(k-1) + \dots + b_p^j u(k-p) \\ &\quad + c_1^j e(k-1) + \dots + c_p^j e(k-p) \\ &\quad + b_0^0 u(k+j) + \dots + b_0^j u(k) \end{aligned}$$

Let s be the number of steps ahead of the prediction. The predicted outputs from time $t = k$ to time $t = k + s - 1$ become:

$$Y_s = AY_p + BU_p + CE_p + PU_s \quad (3)$$

The arrays and the matrices in Equation 3 are obtained by stacking the equations of the output at the above mentioned time steps, i.e. Y_s contains the predicted output at s future time steps from the current one; Y_p , U_p and E_p contain the (measured) outputs, inputs and errors at the previous p time steps, being p the order of the system, and thus are known; U_s contains the control inputs that must be determined to obtain the desired behaviour. The predicted output should be equal to a desired sequence of values, namely $Y_s = Y_d$, resulting in:

$$Y_d = AY_p + BU_p + CE_p + PU_s \quad (4)$$

Generalised Predictive Control. The so called *Minimum Variance Control* [2] descends from Equation 4 by directly imposing the desired output and solving with respect to the required control input. Under the assumption that the system has a direct transmission term (namely, matrix b_0 is invertible) and provided that it is minimum phase, one prediction step is sufficient. Moreover, the response follows the desired behaviour regardless of the required control effort, except for the (unpredictable, because uncorrelated by assumption) error $e(k)$. As a consequence, the variance of the error is minimal. The *Generalised Predictive Control*, on the other hand, represents an extension and a generalisation of this behaviour. The control still tries to force the system to follow the desired output starting from the current step, but the desired behaviour is imposed over a higher number of steps ahead. A prediction horizon higher than the control one can be used; in this case the desired response is imposed in a least square sense. Moreover, the control effort is accounted for by weighting the control output against the prediction error, to avoid saturation of the actuators and/or a rough behaviour. Another form of predictive control is called *Deadbeat Control* [12]. It has not been considered in this work since it can be obtained as a special case of a more general

formulation of the GPC (the same applies to the Minimum Variance), and because it resulted less efficient than the GPC itself, at least in the investigated case. The control output results from the minimisation of the functional

$$J = (Y_d - Y_s)^T (Y_d - Y_s) + \lambda U_s^T U_s$$

with respect to the control input U_s , yielding:

$$U_s = (P^T P + \lambda I)^{\dagger} P^T (Y_d - AY_p - BU_p - CE_p)$$

where λ is the control weight coefficient. The control input at time $t = k$ is given by:

$$u(k) = \alpha_c Y_p + \beta_c U_p + \gamma_c E_p + \delta_c Y_d$$

where δ_c is the last block-row of matrix $Q = (P^T P + \lambda I)^{\dagger} P^T$, and the feedback matrices are $\alpha_c = -\delta_c A$, $\beta_c = -\delta_c B$ and $\gamma_c = -\delta_c C$.

Physical Interpretation of the Predictive Control. The minimum variance control clearly represents a form of zero-pole cancellation. The control cancels the system poles and zeroes by inverting the system $A^{-1}B$. This operation is permitted only if the system is stable and minimum phase, and the resulting close-loop system statically responds to the current, unpredictable input only. The GPC attenuates this effect by simply shifting the poles and zeroes of the system towards higher frequencies. By properly choosing the coefficient λ , both non-minimum phase and unstable systems can be controlled, with limited loss in performances. The choice of the model order and of the prediction and control horizons are key to the effectiveness of the control. The order p must be high enough to account for all the meaningful poles of the system (a rule of thumb says that $p \times m$ should be equal to or slightly higher than the number of poles). But too high an order could result in a poor, and time consuming, identification. The prediction horizon s must be as high as p to ensure that the complete dynamics of the system is accounted for; higher prediction horizons do not add further information to the prediction, but, together with a smaller control horizon, result in an overcollocated enforcement of the desired behaviour, thus overconstraining, and implicitly reducing, the control effort.

Multi-Body Model

A multi-body formulation has been used to describe the dynamics of the tiltrotor. The

equilibrium equations of each node are written; lumped inertia is associated to each node. The bodies are connected by kinematic and dynamic joints. The former are written as algebraic equations that add reaction forces and couples as unknowns, while the latter directly participate in the equilibrium equations by adding configuration-dependent forces. An important example of dynamic constraint is represented by the beam element. Initial value problems are considered, by time integrating the resulting Differential-Algebraic Equation (DAE) system from an initial compatible and *a la d'Alembert* balanced configuration. A Predictor-Corrector integration scheme is used, based on an original formulation that ensures second order accuracy and linear $A-L$ stability, with tunable algorithmic damping [7].

Kinematics. The basic unknowns are represented by the positions and the reference frames of the nodes. The total positions x are used as nodal translational unknowns. Finite rotations are intrinsically nonlinear and require a special treatment in multi-body formulation kinematics. The rotations are described by means of the Gibbs-Rodrigues rotation parameters in a modified *Updated Lagrangian* scheme, called *Updated-Updated* [7], that assumes the predicted configuration as reference. The unknown rotation parameters account for the correction only, and can be considered truly “small”, provided the prediction is accurate. The rotation matrix R , as function of the rotation parameters g , is:

$$R = I + \frac{4}{4 + g^T g} \left(g \times + \frac{1}{2} g \times g \times \right)$$

where the \times represents the cross product between vectors, such that $a \times$ is the matrix that multiplied by b gives $a \times b$. In case of an updated scheme, the total rotation at time $k + 1$ is $R_{k+1} = R(g) R_k$ and in the updated-updated approach it reads $R_{k+1} = R(g) R_{k+1}^0$, where the superscript 0 refers to the predicted value of R at time $k + 1$. The differentiation of a vector that is constant in the local frame gives the expression of the rate of change of the rotation: $v' = R' R^T v = (G g') \times v$, where

$$G = \frac{4}{4 + g^T g} \left(I + \frac{1}{2} g \times \right)$$

The angular velocity is $\omega = G(g) \dot{g}$; in updated-updated form it is $\omega = G(g) \dot{g} + R(g) \omega^0$. Both matrices R and G , as well as other entities

that depend on the rotation parameters such as the angular velocity and those that are used in the linearisation of the kinematic quantities, assume a particularly simple expression when g is zero: both R and G become the identity matrix, the angular velocity becomes $\omega \cong \dot{g} + \omega^0$, while ΔG is zero. Since the unknown updated-updated rotation parameters are small, the simplified expressions are used to speed up the computation of the Jacobian matrix used in the correction iterations, while the residual is consistently computed by using the complete expressions to ensure the accuracy.

Dynamics. The equilibrium equations are written in terms of the derivatives of the momenta β, γ :

$$\begin{cases} \dot{\beta} = F \\ \dot{\gamma} - (\omega \times S) \times \dot{x} = M \end{cases}$$

where S is the first order inertia moment and F, M are generic forces and moments. The definitions of the momenta must be added:

$$\begin{cases} m \dot{x} + S \times \omega = \beta \\ -S \times \dot{x} + J \omega = \gamma \end{cases}$$

m, J being the mass and the second order inertia moment.

Constraint Equations. A kinematic constraint is a relationship between kinematic unknowns. Examples of basic constraints are the coincidence and orthogonality constraints, that can be used to build more complex cases. They result in algebraic or differential equations, depending on whether the constraint is or is not holonomic. A reaction force or couple is required to enforce the constraint. A *Lagrangian Multipliers*-like approach is used. The reactions are directly used as unknowns instead of the multipliers, to avoid the need of postprocessing to determine their value.

Finite Volume Beam. The finite volume beam results from the direct writing of the equilibrium of a finite piece of beam in terms of the internal forces at the boundaries and of the external loads. The internal forces and moments are expressed as functions of the spatial gradient of the configuration by means of arbitrary 6×6 constitutive laws, resulting in a C^0 formulation. The generalised deformations of the beam at the boundary sections result from the differentiation of a linear interpolation of the nodal positions and rotation parameters.

From a mathematical standpoint, the finite volume beam descends from a weighted residuals weak form of the differential equilibrium equation of the beam, with piecewise constant weighting functions. Advantages of the finite volume approach are the ease in the determination of the contribution to the equilibrium equations (only collocated evaluation of the forces is required), the absence of shear locking without the need of any numerical adjustment, and a more intuitive, physical meaning of the contribution to the equilibrium equations. A three-node beam element has been implemented [6].

Tiltrotor Model. The system under analysis is represented by a multi-body analytical model of the Wing and Rotor Aeroelastic Testing System (WRATS) tiltrotor aeroelastic wind-tunnel model. It is a semispan model of the V-22 currently used at LaRC to investigate the tiltrotor technology; it was originally built for the preliminary and full-scale design of the V-22. The analytical model, Figure 1, is made of a three blade, hingeless rotor mounted on a pylon, that is elastically attached to the clamped half-wing. The rotor blades are modelled by 4 beam elements each, plus one beam element for each flexbeam. The complete control chain has been modelled, from the swashplate to the blades through the flexible control links and the pitch horns. The hub is linked to the mast by means of a gimbal joint, that allows the flapped hub to maintain a constant rotation speed both in terms of amplitude and direction. The correct modelling of the gimbal required seven basic joints and one extra body. The analytical model has been validated in terms of kinematic, structural and aerodynamic properties [7]. The kinematic analyses have been used to assess the correct kinematic couplings between blade pitch, flap and lag. Some of these couplings involve the flexibility of the flexbeam and of the control chain, and required to be calibrated directly from the physical model. Structural properties have been compared to analytical results from Bell Helicopter, from previous analyses by means of University of Maryland Advanced Rotorcraft Code (UMARC) and NASTRAN, and to experimental results from Ground Vibration Tests (GVT) performed at LaRC. Basic aerodynamic and aeroelastic validation has been performed by comparing to data from previous wind-tunnel tests and numerical simulations.

Table 1: 888 rpm, $\theta_{75\%} = -3$ deg, Hz

Mode	Myklestad	UMARC	MBDyn
Gimbal	-	14.8	14.8
Cone	17.2	17.3	17.5
1 Lag	22.4	20.8	24.0
Coll Lag	42.	44.0	36.0
2 Flap	37.33	49.6	41.0
2 Flap asym.	-	70.2	65.0
3 Flap	75.33	90.3	73.0
Flap/Torsion	89.33	92.7	90.0
Lag/Torsion	-	113.4	104.0
Torsion	-	116.0	110.0

Numerical Results

Model Validation. Each component of the model has been validated separately. Both non-rotating and rotating analyses have been performed. Good agreement with numerical and experimental data has been found. The relatively rough discretisation used for the rotor blade has been able to capture all the desired modes. The full rotor vibration analysis highlighted the limits of conventional modal analysis of a single blade, since the gimbal joint and the three blade configuration break the symmetry the single blade analyses usually rely on. The UMARC code has been modified to model the three blades in the modal analysis phase, and it confirmed the results of the multi-body analysis. A comparison of modal analysis results is presented in Tables 1 and 2, referring to the rotating frequencies at 888 and 742 rpm, that correspond to the hover and cruise rotating speeds. More exhaustive results of the analysis may be found in Ref. [7].

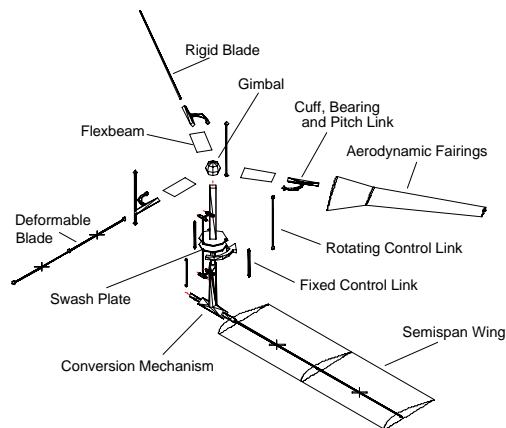


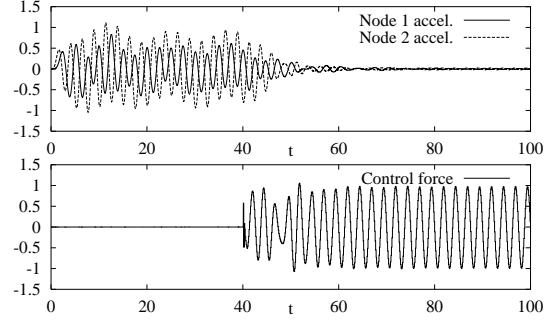
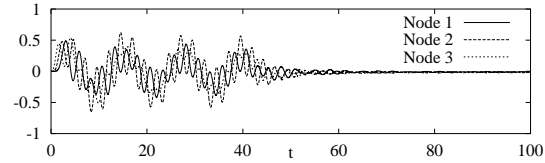
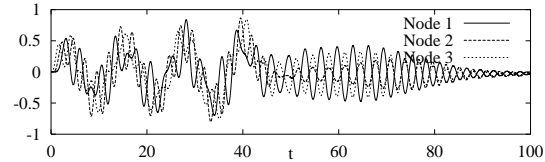
Figure 1: Analytical Model

Table 2: 742 rpm , $\theta_{75\%} = 55 \text{ deg}$, Hz

Mode	Myklestad	UMARC	MBDyn
Gimbal	-	12.4	12.6
Cone	14.7	14.9	15.1
1 Lag	15.3	15.8	16.5
2 Flap asym.	-	42.3	44.2
Coll Lag	32.7	45.9	46.9
2 Flap	45.3	45.6	49.1
3 Flap asym.	-	46.9	60.3
3 Flap	66.0	60.1	65.2
Flap/Torsion	89.3	90.6	97.8
Lag/Torsion	90.0	90.8	89.7
3 Lag	-	92.0	92.9
Torsion	-	116.0	108.5

Control Validation. A very simple system from Ref. [11] is studied. It is made of three masses in series with three springs and dampers; an excitation force is applied at the free end, and the control measures are the accelerations at the other two points, thus implementing a system with no direct transmission term. The properties are: $m_1 = m_2 = m_3 = 1$, $k_1 = 1$, $k_2 = 2$, $k_3 = 3$; the damping is assumed proportional to the square root of the stiffness, i.e. $c_i = 0.05\sqrt{k_i}$. The system has 6 poles. Different values for the order of the identified system p as well as for the control weight λ have been tested. The prediction and control advancing horizons have been chosen equal to p . The integration time step is 0.01 s; the sampling for the discrete controller is taken every 10 time steps. The system is excited by a unit amplitude harmonic force at 0.4 Hz; a white noise with 0.001 amplitude is applied and measured to identify the system. The control is activated after 40 s of simulation. An order $p = 6$ has been used, with $\lambda = 10^{-3}$. The control weight is gradually lowered to the nominal value in about ten seconds to avoid an abrupt intervention of the control. Figures 2, 3 show the two measured accelerations and the control force, and the displacements at the three nodes, respectively. When the first damping coefficient is set to a negative value $c_1 = -0.15\sqrt{k_1}$, the response, Figure 4, shows the effectiveness of this form of adaptive control for unstable systems. It is interesting to note that the control is not collocated and the unstable section of the system is close to one of the measures, but not directly controllable. The control weight λ can be reduced even more, with performance improvements especially in the unstable case, but with excessive penalty in

the required control force.


 Figure 2: *3 Masses — Control Signals*

 Figure 3: *3 Masses — Displacements*

 Figure 4: *3 Masses — Unstable Displacements*

Hover Simulations. The effectiveness of the GPC applied to a more complex and realistic system has been assessed by performing simple SISO control analyses of the WRATS model in hover. The rotor is rotating at 888 rpm, and it is externally excited by a shaker with a harmonic load at 5 Hz, close to the first wing out-of-plane bending frequency, about 5.5 Hz. The time step is 0.001 s, and the control samples are taken every 8 steps, resulting in a frequency of 125 Hz, which is higher than the first torsional frequency of the blade, to prevent the blade resonance. The bending strain at the root of the wing is measured, filtered by a washout (band-pass) analog filter to cut out of the measured signal the static signal as well as the higher frequencies, and the rotor thrust is used as actuator by controlling the collective pitch. A pass-band filtered measure of the vertical acceleration at the pylon is alternatively used. A good compromise for the system order has been found in $p = 60$. The

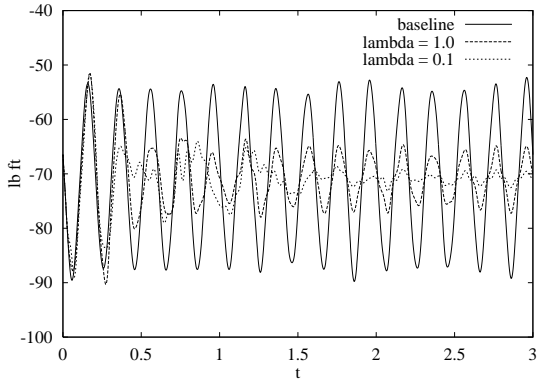


Figure 5: *Hover bending moment, str. meas.*

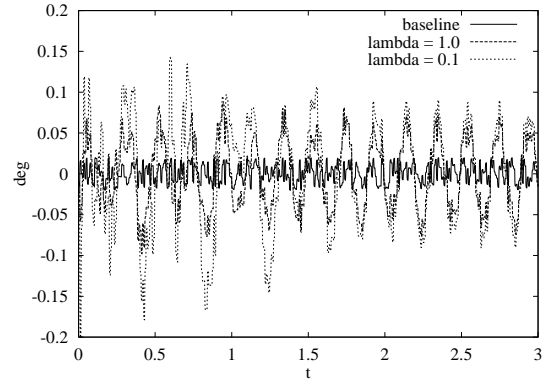


Figure 7: *Hover collective, str. meas.*

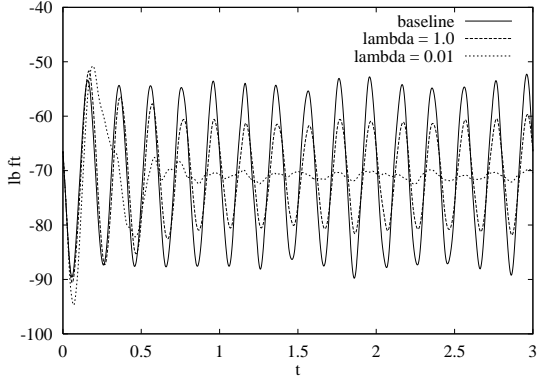


Figure 6: *Hover bending moment, acc. meas.*

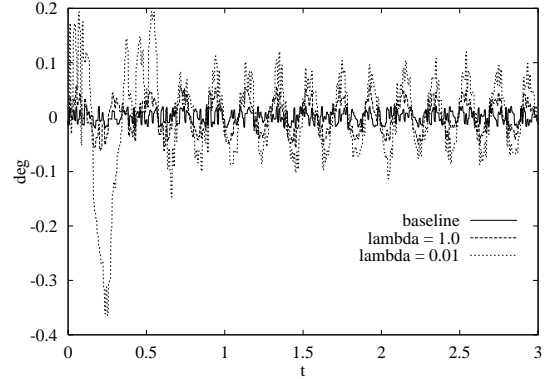


Figure 8: *Hover collective, acc. meas.*

results of the two cases, compared to a baseline analysis with harmonic excitation but without control, are presented in Figures 5, 6, for two different values of λ . They show the bending out-of-plane moment at the wing root. The control signals are shown in Figures 7, 8, while the vertical acceleration of the pylon in the latter case is shown in Figure 9; the high frequency noise is the persistent excitation that is used to continuously identify the system, while the control of the harmonic motion determines the main, low frequency oscillation.

Forward Flight Simulations. Forward flight analyses have been performed by controlling the collective and the cyclic pitch of the blades based on different measures of strains at the wing root. The model is in airplane configuration, at an airspeed of 100 ft/s, and the rotor is rotating at 742 rpm. In this case the order is $p = 20$, since the number of measures is higher (3 vs. 1). First the wing out-of-plane excitation force is offset aft of the wing to obtain also a twisting excitation. The rotor has little control authority in its plane in terms of force, the flapping of the

disk being required to tilt the thrust. Since the flapping response has a delay of about 90° , the accuracy of the prediction is key to the effectiveness of the control. In this case the actuation force, transverse to the wing, lies in the plane of the rotor, thus being not directly controllable by a simple change in thrust. Moreover, since the motion of the gimbaled rotor is characterised by a wide spectrum dynamics, from the high frequency vibrations induced by the advancing blade modes, to the wing elastic modes, down to the very low frequency precession motion, a high number of physical and numerical poles are required for an adequate identification. The results of the simulations are reported in Figure 10, that shows the wing root bending moment. Figure 11 shows the control signals. The initial low frequency oscillations in the control signals are due to the precession of the rotor during the transient following the application of the harmonic excitation. The uncertain initial behaviour of the controller is related to a poor initial identification of the low frequency poles of the system. In fact, with $\lambda = 1.0$ the control authority is low, but with $\lambda = 0.1$, after a

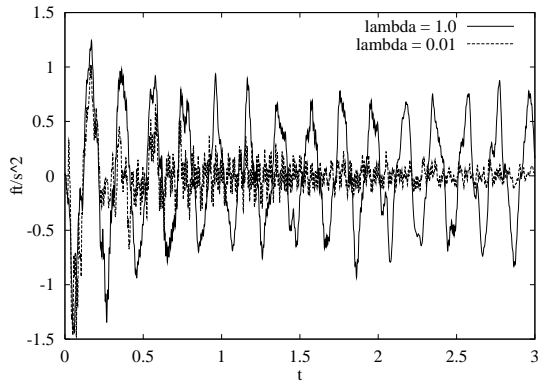


Figure 9: *Hover accelerometer signal*

few cycles the system goes slightly unstable (after about 1.5 s), returning under control as soon as the identification is improved. The following behavior is definitely better than the previous case, as can be appreciated in the last part of the plot. A more realistic case is considered, by using the control parameters tuned with the former case. A cosinusoidal vertical gust, with an amplitude of 4 ft/s and a wavelength of 20 ft, is encountered by the model while the control is working. The effect of the control on the wing bending is shown in Figure 12: the free oscillations resulting from the wind-up of the rotor are damped as the control starts; when the model encounters the gust, the peak of the moment is attenuated first, then the control overshoots due to the need to re-identify the system. The newly identified system brings the bending moment, as well as the other measured internal moments, to a negligible value in a few cycles. The control signals, i.e. the pitch controls determined by the controller, are particularly meaningful. The col-

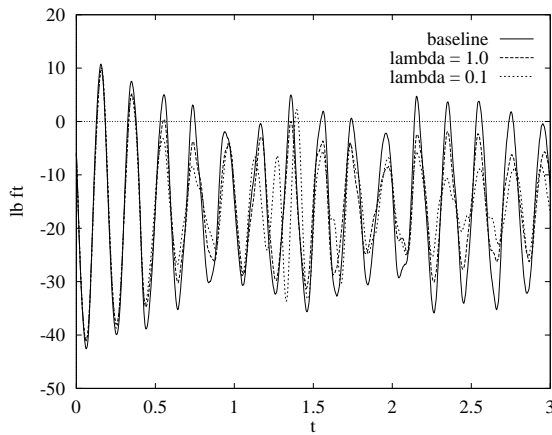


Figure 10: *Forward flight bending*

lective is negligible, since it mainly controls the in-plane bending of the wing, that is not directly excited by the vertical gust. The cyclic controls instead are heavily used by the controller to generate the rotor aerodynamic moment required to tilt the rotor disk. Since the disk tilts about an horizontal axis due to the wing bending and torsion excited by the gust, the rotor is mainly required to generate a pitch moment (in airplane sense) that counteracts this motion. In fact the higher cyclic control signal is the lateral pitch, about twice as large as the fore/aft pitch, which causes a fore/aft flapping of the rotor. Figure 13 shows a detail of the control signals across the gust input.

Concluding Remarks

The Generalized Predictive Control has been used in the multi-body numerical simulation of the active vibration control of a tiltrotor aeroelastic model currently investigated at NASA Langley Research Center. The control has been applied by means of the control mechanism that is used on the actual model, a conventional, hydraulically actuated swashplate. A combination of strain and acceleration measures have been used to identify the system, and different operating conditions and external disturbances have been considered. The predictive control resulted highly effective in most of the investigated conditions, giving substantial reduction of the load level. In detail, both the strain and the acceleration measurements allowed the correct identification of the system, and the intrinsic adaptivity of the proposed implementation of the generalised predictive control allowed the correction of inaccurate initial system identification even

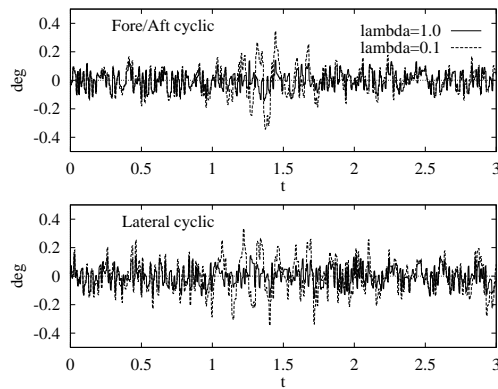


Figure 11: *Forward flight control signals*

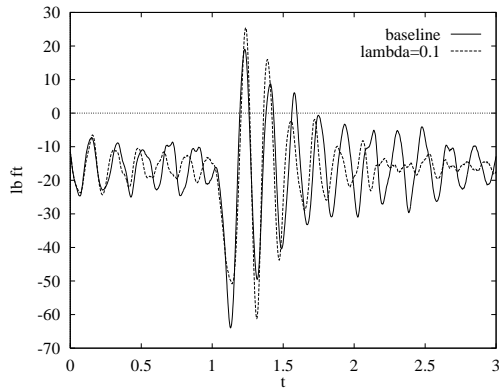


Figure 12: *Gust bending*

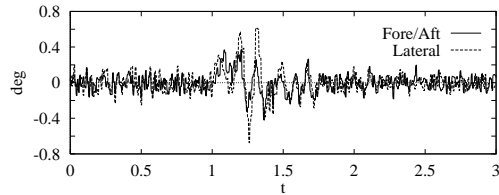


Figure 13: *Gust control signals*

in variable test conditions. The multi-body approach represented a viable solution for the analysis of complex systems requiring a high level of detail in the modelling of mechanisms. Future developments of the control will involve the introduction of the adaptivity of the weight coefficient, to reduce the need of an *ad hoc* tuning of the various control parameters, and a variable order model in the identification of the system.

References

- [1] Andrighettoni, M., and P. Mantegazza, 1998, "Multi-Input/Multi-Output Adaptive Active Flutter Suppression for a Wing Model", *Journal of Aircraft*, Vol. 35, No. 35, pp. 462-469
- [2] Åstrom, K. J., and B. Wittenmark, 1989, *Adaptive Control*, Addison-Wesley
- [3] Chopra, I., and J. L. McCloud, 1981, "A Numerical Simulation Study of Open-Loop, Closed-Loop and Adaptive Multicyclic Control Systems", Presented at the *American Helicopter Society Northeast Region National Specialists' Meeting on Helicopter Vibration, Technology for the Jet Smooth Ride*, Hartford, Conn.
- [4] Eure, K. W., and J. Juang, 1997, "Broadband Noise Control Using Predictive Techniques", *NASA TM 110320*
- [5] Friedmann, P. P., and T. A. Millot, 1995, "Vibration Reduction in Rotorcraft Using Active Control: a Comparison of Various Approaches", *J. of Guidance, Control, & Dynamics*, Vol. 18, No. 4, July-August
- [6] Ghiringhelli, G. L., P. Masarati, and P. Mantegazza, 1997, "Multi-Body Aeroelastic Analysis of Smart Rotor Blades, Actuated by Means of Piezo-Electric Devices", *CEAS Int. Forum on Aeroelasticity and Structural Dynamics*, June 17-20, Rome, Italy
- [7] Ghiringhelli, G. L., P. Masarati, P. Mantegazza, and M. W. Nixon, 1998, "Multi-Body Analysis of a Tiltrotor Configuration", Presented at the *7th Conference On Nonlinear Vibrations, Stability, and Dynamics of Structures*, July 26-30, Blacksburg, VA; to be published on the *J. of Nonlinear Vibrations*
- [8] Giurgiutiu, V., Z. Chaudry, and C. A. Rogers, 1995, "Engineering Feasibility of Induced Strain Actuators for Rotor Blade Active Vibration Control", *JoIMS&S*, Vol. 6, September
- [9] Ham, N. D., 1987, "Helicopter Individual-Blade-Control Research at MIT 1977-1985", *Vertica*, Vol. 11, No. 1/2, pp. 109-122
- [10] Johnson, W., 1982, "Self-Tuning Regulators of Multicyclic Control of Helicopter Vibrations", *NASA TP 1996*
- [11] Juang, J., 1997, "State-Space System Realization With Input- and Output-Data Correlation", *NASA TP 3622*
- [12] Juang, J., and M. Q. Phan, 1997, "Deadbeat Predictive Control", *Journal of the Chinese Society of Mechanical Engineers*, Vol. 19, No. 1, pp. 25-37
- [13] Lehmann, G., 1985, "The Effect of Higher Harmonic Control (HHC) On a Four-Bladed Hingeless Model Rotor", *Vertica*, Vol. 9, No. 3, pp. 273-284
- [14] Loewy, R. G., 1984, "Helicopter Vibrations: A Technological Perspective", *Journal of the American Helicopter Society*, October, pp. 4-30
- [15] Nixon, M. W., R. G. Kwaternik, and T. B. Settle, "Higher Harmonic Control Tiltrotor Vibration Reduction", *CEAS Int. Forum on Aeroelasticity and Structural Dynamics*, June 17-20 1997, Rome, Italy
- [16] Reichert, G., 1981, "Helicopter Vibration Control - A Survey", *Vertica*, Vol. 5, N0. 1, pp. 1-20